Cell Tissue Res (1998) 294:485-501

REGULAR ARTICLE

Ulrich Welsch · Friedrich Feuerhake · Rudi van Aarde
Wolfgang Buchheim · Stuart Patton

Histo- and cytophysiology of the lactating mammary gland of the African elephant (*Loxodonta africana)*

Received: 22 May 1998 / Accepted: 13 July 1998

Abstract The lactating mammary gland of the African elephant *(Loxodonta africana)* has been studied with a panel of morphological techniques focusing on (1) the functional changes during the secretory process, (2) proliferative process [by application of proliferating cell nuclear antigen (PCNA) immunohistochemistry] and apoptotic phenomena [by use of the TUNEL technique] in the individual lobules, and (3) components of milk and milk-fat-globule membrane. In the lactating gland, the lobules are variably differentiated; within a lobule, however, the alveoli are usually similarly differentiated. The morphology of their alveoli suggests a classification of the lobules into types 1–3. Lobules of type 1 are composed of immature tubular alveoli with mitotic figures and numerous PCNA-positive nuclei; advanced type 1 alveoli contain abundant glycogen and specific secretory granules. Lobules of type 2 are further subdivided. In type 2a lobules, the epithelial cells of the alveoli form tall apical protrusions, which in part are occupied by small lipid droplets and which are pinched off in an apocrine fashion. The number of lysosomes varies considerably. Type 2b is the most common type, with striking basal membrane foldings, abundant rough endoplasmic reticulum cisterns, large Golgi apparatus, numerous mitochondria, lipid droplets, and protein vesicles with 30- to 90-nm-wide casein micelles. The lipid droplets are pinched off with minimal amounts of cytoplasm. Type 2c is composed of alveoli with a cuboidal epithelium and few signs of secretory activity. Increasing expression of peanut-agglutinin-binding sites parallels the maturation and differentiation of the glandular cells. Type 3 lobules are marked by numerous TUNEL-positive nuclei and large lipid droplets and are apparently degenerating structures. Cytokeratin (CK) 14 is usually present in the myoepithelial cells; CK 19 and CK 7 mark ductal and immature alveolar epithelia. Milk protein content varies between 2.6% and 6.3%, and casein micelles range from 35 to 90 nm in diameter. The diameter of intra-alveolar milk fat globules ranges from 5 to 25 µm and the membranes bear a filamentous surface coat composed of membrane-anchored mucins; gel-electrophoretic analysis of these mucins from different individuals demonstrates the presence of mucin MUC 1, which is expressed with considerable genetic heterogeneity.

Key words Mammary gland · Lactation · Secretion · Proliferation · Apoptosis · Milk · African elephant, *Loxodonta africana* (Proboscidea)

Ulrich Welsch (✉) · Friedrich Feuerhake
Anatomische Anstalt, Lehrstuhl II, Universität München,
Pettenkoferstrasse 11, D-80336 München, Germany
Tel.: +49–89–5160 4820; Fax: +49–89–5160 4897
e-mail: welsch@anat.med.uni-muenchen.de

R. Van Aarde
Mammal Research Institute, University of Pretoria, Pretoria, RSA

W. Buchheim
Bundesanstalt für Milchforschung, University of Kiel,
Kiel, Germany

S. Patton
Center of Molecular Genetics, University of California,
San Diego, USA

Introduction

The aim of the present study has been to analyze, by various light-microscopical and electron-microscopical techniques, the functional organization of the lactating mammary gland in the African elephant (*Loxodonta africana*) with emphasis on the secretory process, changes in functional activity, and proliferative and apoptotic phenomena in a mammary gland that produces milk for an unusually long period (see below).

Lactation is an important part of the postnatal development and the reproductive biology of any mammal (see Mepham 1987). A fuller understanding of the various aspects of the reproduction of the African elephant (*Loxo donta africana*) is particularly important because of necessary decisions for conservation of this the largest terrestrial mammalian species and for taking measures against over-

Table 1 Lectins used for the present study

Lectin	Abbreviation	Nominal sugar specificity
Helix pomatia agglutinin	HPA	*N*-acetylgalactosamine
Peanut agglutinin	PNA	Galactose
Wheat germ agglutinin	WGA	*N*-acetylglucosamine
Canavalia ensiformis agglutinin	ConA	Mannose, glucose
Ulex europaeus I agglutinin	UEA I	Fucose
Ricinus communis I agglutinin	RCA I	β-Galactose, *N*-acetylgalactosamine

population in the artificial situation present in enclosed game reserves (Greyling et al. 1997).

According to Perry (1953), the lactation of the African elephant usually lasts 18–24 months but can often extend over 4 years; single observations have even shown that, in individual animals, lactation can continuously occur throughout reproductive life. In a typical herd, which essentially consists of a leading female (matriarch) and her daughters with offspring (Skinner and Smithers 1990), a calf can be nursed by both mother and aunts. The average birth weight of an elephant is about 120 kg (Laws 1969), and its rate of growth during suckling is, as in other large placental mammals, slower than in small placental mammals. Interestingly, large terrestrial mammals appear to produce less concentrated milk than small mammals (McCullagh and Widdowson 1970).

So far, no modern study on the mammary gland of the African elephant exists, and it seems worthwhile to study the mammary gland of an animal that lactates continuously over such a long period. Laboratory rodents are the mammals that are usually studied as models for lactation, differentiation, and degeneration of the glandular tissue (Dulbecco et al. 1983; Joshi et al. 1986; Walker et al. 1986; Humphreys et al. 1996; Li et al. 1997), and these animals lactate only for a short period, usually 2–3 weeks; during this short time, the lactating glandular tissue is of a uniform appearance. It is of interest to know whether morphological and histochemical correlations with the long lactation period can be detected in the mammary gland of the elephant.

With respect to the percentage of the main components of the milk of the African elephant, the following basic information is available: water, 80%; protein, 5.1%; lactose, 3.6%; lipid, 9.3%, ash, 0.7% (McCullagh and Widdowson 1970). More information on this milk is desirable because of the remarkable difficulties associated with the artificial rearing of elephant calves from birth in captivity (McCullagh and Widdowson 1970). No data exist to date on the structural organization of lactating glandular cells or on physical parameters, e.g., the size of milk fat globules and casein micelles, which are important for the digestive process (Jensen et at. 1995). In view of the available data on mucins associated with milk-fat-globule (MFG) membranes (MFGM) of various primates, horses, bovids, and carnivores (Welsch et al. 1988, 1990; Patton et al. 1989, 1995; Patton and Patton 1990), it is of additional interest to compare these morphological and biochemical data with new observations on these macromolecular components in elephant's milk. The expression of these mucins is genetically polymorphic (Patton et al. 1995), which offers the opportunity to use them for studies of population genetics.

Materials and methods

Lactating mammary tissue and milk samples were collected from 12 adult female elephants shot for necessary management purposes in the Kruger National Park, South Africa, during April and May 1993, as an extension of the study on estrogen and progesterone receptors in *Loxodonta* (Greyling et al. 1997). Principles of animal care and specific national laws were followed. Five to ten minutes after death, tissue samples were excised for light and electron microscopy from various sites of the gland and about 30–50 ml milk was collected from each animal.

Light microscopy

Pieces of tissue measuring 1–2 cm in diameter were taken from various locations of the gland, fixed in phosphate-buffered formalin, and embedded in Paraplast. Sections (5–6 µm thick) were stained with hematoxylin-eosin, Masson's trichrome stain, resorcin fuchsin, and Alcian blue (pH 1 and 2.5), and with the PAS and Feulgen reactions (Feulgen and Rossenbeck 1924; Romeis 1989).

Table 1 lists the lectins applied to paraffin sections for the visualization of specific carbohydrates (see Wu and Herp 1985). The lectins were obtained from Medac (Hamburg, Germany) and Sigma (Deisenhofen, Germany). For controls, they were used with their inhibitory sugar.

Immunohistochemistry for the demonstration of cytokeratins (CK) was performed by using the following working dilutions of monoclonal antibodies to the relevant human proteins: anti-CK 7 (DAKO, Glostrup, Denmark), 1:100, anti-CK 14 (Serotec, UK) 1:10, anti-CK 19 (Boehringer Mannheim, Germany) 1:20. Sections were

Fig. 1a–k Light microscopy of the lactating mammary gland of the African elephant. **a–c, f,g,i** Paraffin sections, **d,e,h,j,k** semithin sections. **a** Low-power micrograph showing the general structure of the lactating gland; hematoxylin-eosin (H.E.). x22. **b** The PAS reaction is strongly positive in a type 1 lobule *(1)* and ductal epithelia *(D)*. x22. **c** Higher magnification of the PAS reaction with advanced alveoli in a type 1 lobule; note the positive reaction in the epithelium and lumen. x110. **d** Lobule type 1 with immature tubular epithelial elements; note the mitotic figure (*arrow*) and large euchromatin-rich nuclei. x440. **e** Lobule type 2a; note the alveoli with tall cells forming a prominent apical protrusion (*arrows*); toluidine blue. x220. ***f*** Lobule type 2a; note the tall eosinophilic apical protrusions (*arrows*); H.E. x220. **g** Small ducts of a type 2a lobule; note the pinched-off apical protrusion (*arrows)* of the secretory cells; H.E. x220. **h** Lobule type 2b; the secretory epithelium is cuboidal, and the lumen contains abundant MFGs; toluidine blue. x220. **i** Lobule type 2c; empty alveoli, cuboidal or flat epithelia, few signs of secretory activity; H.E. x110. **j** Lobule type 3; the epithelial cells contain large fat droplets, and the epithelial wall shows in part indications of disintegration. x230. **k** Small intralobular duct with areas of transition between ductal and alveolar epithelium (*arrows*). x220

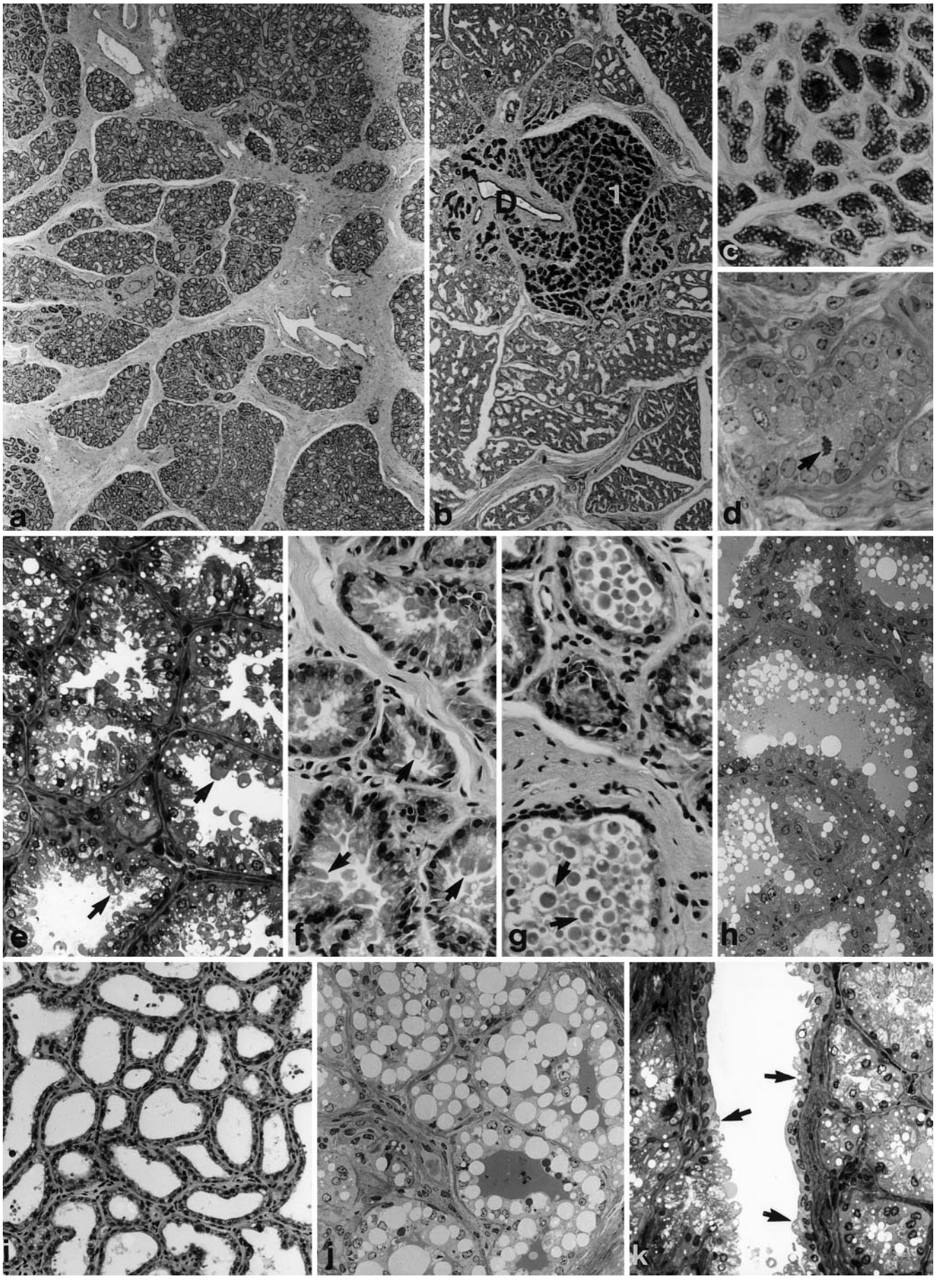
a
b
D
1
c
d
e
f
g
h
i
j
k

Table 2 Staining results with the PAS reaction (+ weak, ++ medium, +++ strong reaction)

	Lobules type 1	Lobules type 2	Lobules type 3	Interlobular ducts
Alveolar epithelium	+++ (entire cytoplasm)	+/++ (apical cell membrane)	+ (apical cell membrane)	+/++ (epithelium)
Non-lipidic material in alveolar lumen	++/+++	–	–	–
Milk fat globule membrane	Usually not present	++/++	+/++	–

Table 3 Staining results with Alcian blue [(+) faint, + weak, ++ medium, +++ strong]

	Lobules type 1	Lobules type 2	Lobules type 3	Interalveolar ducts
Alcian blue, pH 2.5	Connective tissue ++/+++ Alveoli –	Connective tissue + Alveoli lumen –/+ Apical membrane often (+) MFG (+)	Connective tissue + Alveoli lumen –/+ Apical membrane –/+ MFG (+)	Connective tissue+ Epithelia –/(+)
Alcian blue, pH 1	Connective tissue + Alveoli –	Connective tissue (+) Alveoli lumen –/(+) Apical membrane –	Connective tissue (+) Alveoli lumen –/(+) Apical membrane –	Connective tissue (+) Epithelia –

pre-incubated with 0.2% trypsin at 37°C for 15 min, except for anti-CK 14, which required antigen retrieval by microwave-heating in citrate buffer at pH 6 for 5 min, twice. Immunoreactivity of the primary antibodies was visualized by using biotinylated goat anti-mouse IgG (Sigma, dilution 1:200 to 1:400), followed by peroxidase-conjugated streptavidin (DAKO) and 3.3 diaminobenzidine (DAB) as the chromogen. The specificity of the primary antibodies was demonstrated in human tissues, such as skin, colon, and bronchus, in which they showed the typical epithelial CK pattern (Moll et al. 1982; Purkis et al. 1990). For all antibodies used, optimal concentrations were determined in dilution series for human and elephant mammary tissues. As a positive control, sections of human mammary gland were treated in exactly the same manner as the elephant sections. Negative controls were performed by replacing the primary antibody with irrelevant mouse antibodies or non-immune-mouse serum.

The TUNEL [terminal transferase (TdT)-mediated d-UTP nick-end-labeling] procedure was performed on dewaxed paraffin sections as described by Gavrieli et al. (1992) with the following modifications. All rinsing steps were performed in phosphate-buffered saline (PBS) at pH 7.4 Proteinase K digestion was replaced by microwave irradiation (1 min, 750 W) in 0.1 M citrate buffer, pH 6.0 Sections were incubated with a blocking reagent (0.1 M TRIS-HCI pH 7.5, 3% bovine albumin, 20% calf serum) for 30 min at room temperature. Endogenous peroxidase was blocked by 0.3% H_2O_2 in methanol for 10 min. Sections were incubated for 1 h at 37°C with TdT and flourescein-conjugated d-UTP (Boehringer Mannheim). For visualization by light microscopy, a peroxidase-conjugated anti-flourescein antibody (Boehringer Mannheim), followed by DAB was used. As positive controls, sections of human and African elephant intestine were treated in the same way. As negative controls, either the enzyme or dUTP was omitted.

The immunohistochemical detection of proliferating cells was performed by using a monoclonal antibody to the proliferating cell nuclear antigen (PCNA, cyclin; DAKO) at working dilution of 1:200. The sections were pretreated with microwave irradiation in citrate buffer at pH 6.0 for 10 min, twice. The primary antibody was detected as described above by using biotinylated goat anti-mouse IgG (Sigma, dilution 1:1000). Sections were counterstained with hematoxylin. Positive controls were performed by using human and elephant small intestine. Negative controls were treated equally by replacing the primary antibody by irrelevant mouse antibodies or non-immune mouse serum. Cross-reactivity tests and dilution series were also performed for antibodies to the Ki-67 antigen (MB-1, Dianova, Germany/Ki-S5, Boehringer Mannheim). These antibodies showed no cross-reaction between human and elephant tissue.

Electron microscopy

Tissue samples measuring 1–2 mm in diameter were fixed in cold 3.5% phosphate-buffered glutaraldehyde for 3 h and thereafter transferred for 6 days into cold 1% phosphate-buffered glutaraldehyde. Before the tissue was embedded in Araldite, the samples were rinsed in phosphate buffer and postfixed in 2% osmic acid. Semithin sections were stained with toluidine blue for general orientation. Thin sections were stained with uranyl acetate (saturated solution in 70% methanol) and lead citrate and examined under a Philips CM 100 electron microscope.

Gel electrophoresis of MFGs

Fat globules were isolated by centrifuging elephant milk through an overlayer of water (Patton and Huston 1986). The final concentration of the purified globules was adjusted to 10%–20% [based on the total lipid weight determined by using the Roese-Gottlieb method (Horwitz 1975)]. Sodium-dodecyl-sulfate/polyacrylamine gel electrophoresis (SDS-PAGR) of globule preparations was performed according to the Laemmli method (Laemmli et al. 1970). The samples were denatured by applying SDS, mercaptoethanol, and heat. They were then centrifuged at 1500 *g* for 20 min, and only the fat-depleted lower phases were electrophoresed. Slab gels (105 mm long, 135 mm wide, and 1.5 mm thick) were used. The top 20 mm was a 3% acrylamide stacking gel, the remainder (85 mm) being 6% running gel. A current of 10 mA, decreasing to 6 mA, was applied for 18 h. The gels were stained for glycoproteins by using the PAS reaction and a silver stain (Morrissey 1981). Protein content of milk samples was determined by the bicinchoninic acid procedure and reagents (Pierce Chemical, Rockford, Ill.) with bovine serum albumin as the standard.

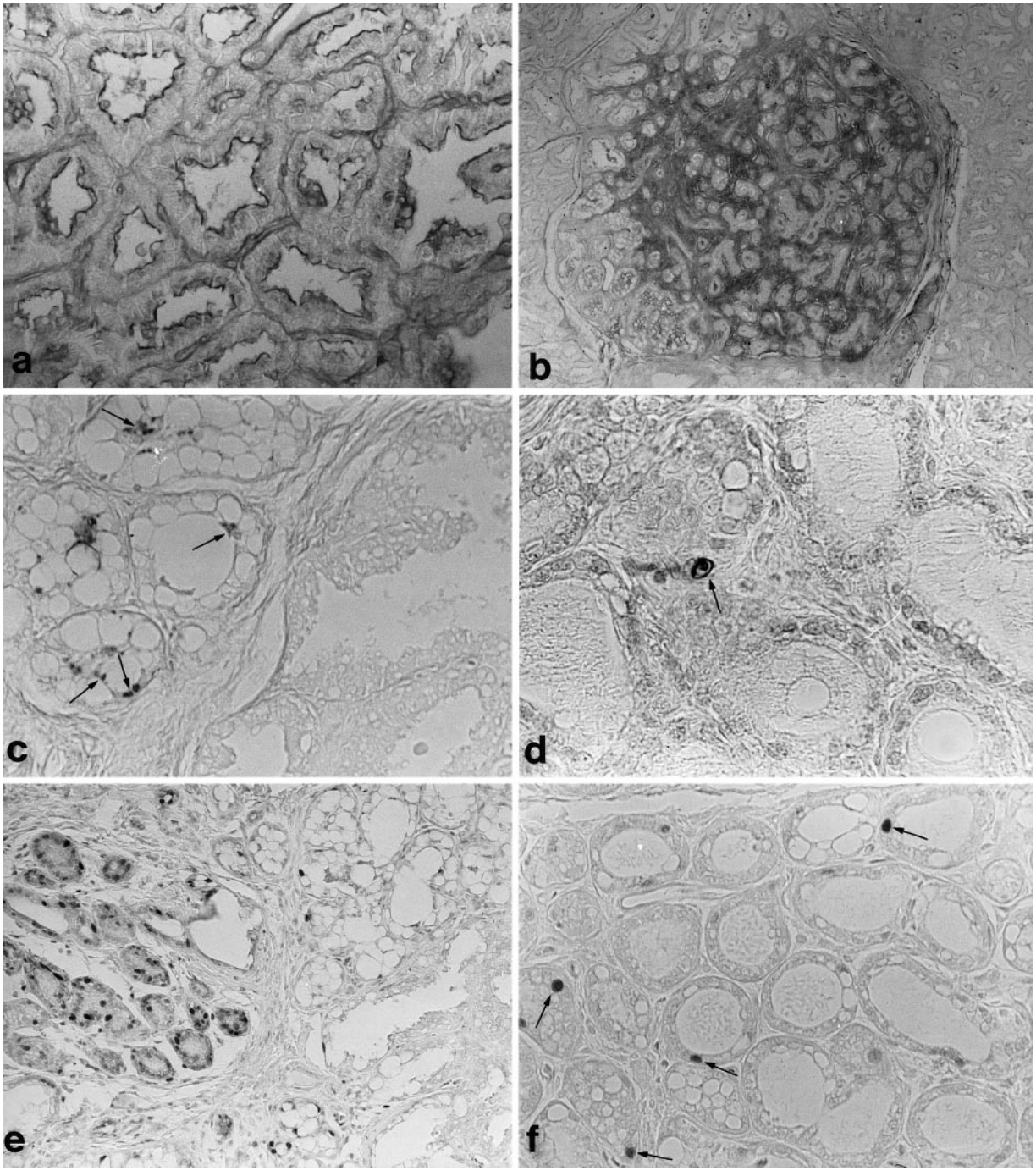

Fig. 2a–f **a** PAS reaction in alveoli of type 2 lobule, marked by a distinct positive reaction at the apical membrane. x220. **b** Type 1 lobule stained with Alcian blue, pH 2.5; note the strong stain of the intralobular connective tissue. x45. **c–f** Proliferation and apoptosis in lactating mammary gland. **c** *Left* Type 3 lobule, showing positive reaction for fragmented DNA (*arrows*); *right* type 2 lobule with negative TUNEL reaction; TUNEL. x180. **d** TUNEL-positive nucleus (*arrow*) showing chromatin condensation and a halo as morphological signs of apoptosis, type 2 lobule; TUNEL. x365. **e** High proliferation activity in a type 1 lobule *(left*), when compared with type 3 and 2 lobules (*right*); PCNA. x90. **f** Single PCNA-positive nuclei *(arrows)*, loosely distributed in a type 2 lobule; PCNA. x180

Freeze-fracture and freeze-etching for electron-microscopic demonstration of the MFGM

Fresh milk samples were mixed with 1% glutaraldehyde and kept cool until further processing. Initially, 35% glycerol was added to the fixed milk samples in order to avoid ice crystal formation, which can cause freezing artifacts. Fat globules were obtained as a layer by centrifugation at 100 *g* for 10 min, followed by three cycles of redispersion in water and recentrifugation to wash the globules. After this washing procedure the temperature of the samples was raised to about 35°C, in order to induce complete fluidity of the milk fat before cryofixation. This ensured frequent fracture plants between the two membrane leaflets. Aliquots of 1–2 µm of the final cream-layer samples were mounted on freeze-fracture specimen holders, cryofixed by immersion in melting Feon 22 (–160°C), freeze-fractured at –105°C, and then etched for 3 min (Balzers BA-360-M unit). The etched specimens were replicated by shadowing with platinum/carbon (2 nm) and backing with pure carbon (20 nm). Further details of the procedure have been given elsewhere (Buchheim 1982a).

Results

Mammary gland

The structural units of the lactating mammary gland at the histological level are variably shaped lobules (diameter about 1.5–2.5 mm, Fig. 1a). The lobules are composed of tubulo-alveolar secretory portions that drain into small intralobular ducts, a leading duct of which leaves the lobule and opens into a large interlobular duct located in the connective tissue septa that separate the individual lobules (Fig. 1a, b). The small intralobular ducts originate without a sharp border from the alveoli (Fig. 1k) and can be best demonstrated by immunohistochemical staining for CK 7 and CK 19 (see Fig. 3e) and also by the PAS reaction (Table 2, Fig. 1b), because of the presence of glycogen. Their epithelial wall is composed of myoepithelial cells and cuboidal epithelial cells with no light-microscopical indications of secretory activity. In the electron microscope, the epithelial cells of the intra- and interlobular ducts can be seen to contain single dense secretory granules, single small lipid droplets, often numerous glycogen particles (predominantly β-particles), and many intermediate filaments (diameter 8–10 nm). Apically, the cells bear numerous variably structured microvilli with a prominent surface coat. Myoepithelial cells form an initially loose and then an increasingly coherent layer of basal cells.

The connective tissue around the interlobular ducts and in the septa separating the lobules contains loosely distributed fibrocytes, small thick-walled arteries (with 8–9 layers of smooth muscle cells), veins (with 2–4 layer of smooth muscle cells), numerous wide lymphatic vessels, small nerves, and single Vater-Pacini bodies. Univacuolar adipocytes form uncommon small cell groups. The predominant connective tissue fibers are collagen fibers. Elastic fibers are present but in smaller numbers. Aldehyde fuchsin-positive fibers are more common than resorcin fuchsin-positive fibers, indicating the existence of oxytalan fibers, as confirmed in electron-microscopical preparations in which bundles of microfilaments are commonly to be found. The interlobular connective tissue septa stain moderately with Alcian blue, the staining intensity of which is stronger at pH 2.5 than at pH 1 (Table 3).

The connective tissue within the lobules stains generally more strongly with Alcian blue, and even more so at pH 2.5 than at pH 1, than in the interlobular septa (Table 3). In type 1 lobules (see below), the Alcian blue stain is particularly strong (Fig. 2b). This intralobular connective tissue contains fibrocytes (Fig. 1f, g), numerous plasma cells (see Fig. 6c), single eosinophils (see Fig. 6c), single lymphocytes, fine collagen fibers, oxytalan fibers, and numerous blood capillaries (see Fig. 6c), but not lymphatic capillaries. The wall of the blood capillaries consists of a continuous endothelium with numerous oval pinocytotic vesicles (see Fig. 6a). The distance between the basal cell membrane of the glandular cells and the basal cell membrane of the capillaries measures 0.8–2 µm. Mast cells are uncommon elements in the connective tissue septa and stain with Alcian blue and metachromatically with toluidine blue. Rarely, small infiltrations of lymphocytes and neutrophils have been observed. The latter have also been detected near and in the epithelial wall and in the lumen of single disintegrating alveoli.

The epithelial component of the lobules consists of densely packed alveoli and the above mentioned small ducts. The wall of the alveoli is composed of secretory epithelial and myoepithelial cells; the latter usually react positively for CK 14. Single lymphocytes can regularly be observed in the epithelium. The shape of the lactating alveoli varies but is usually similar within a single lobule. Preliminarily, three types of lobules can be distinguished.

Type 1

This type is marked by small tubular profiles with a narrow lumen, or even without a lumen, measuring 30–60 µm in diameter (Fig. 1b), all of which are regarded as representing immature ductular and secretory units; more advanced secretory units with a wider lumen also sometimes occur in such lobules (see below). The glandular cells of the immature epithelial structures only occasionally contain small lipid droplets; their nuclei are large and rich in euchromatin and possess 1–2 nucleoli per section. Single mitotic figures have been observed regularly in these lobules (Fig. 1d). The number of proliferating cells as detected by PCNA is clearly increased compared with all other types of lobules (Fig. 2e). The epithelial cells of type 1 lobules express CK 7 and CK 19, which are both characteristic for the ductal phenotype of epithelial cells (see above; Fig. 3e). The cytoplasm is strongly PAS-positive (Fig. 1b, c); this corresponds to abundant glycogen particles as can be seen in the electron microscope (see Fig. 5a). Furthermore, the glandular epithelial cells are marked by numerous free ribosomes, several cisternae of rough endoplasmic reticulum (RER), small mitochondria, and a medium-sized supranuclear Golgi apparatus giving rise to single secretory granules that presumably contain protein and will be termed, in accordance with the corresponding structures of more mature lobules, protein vesicles. Such protein vesicles become more frequent

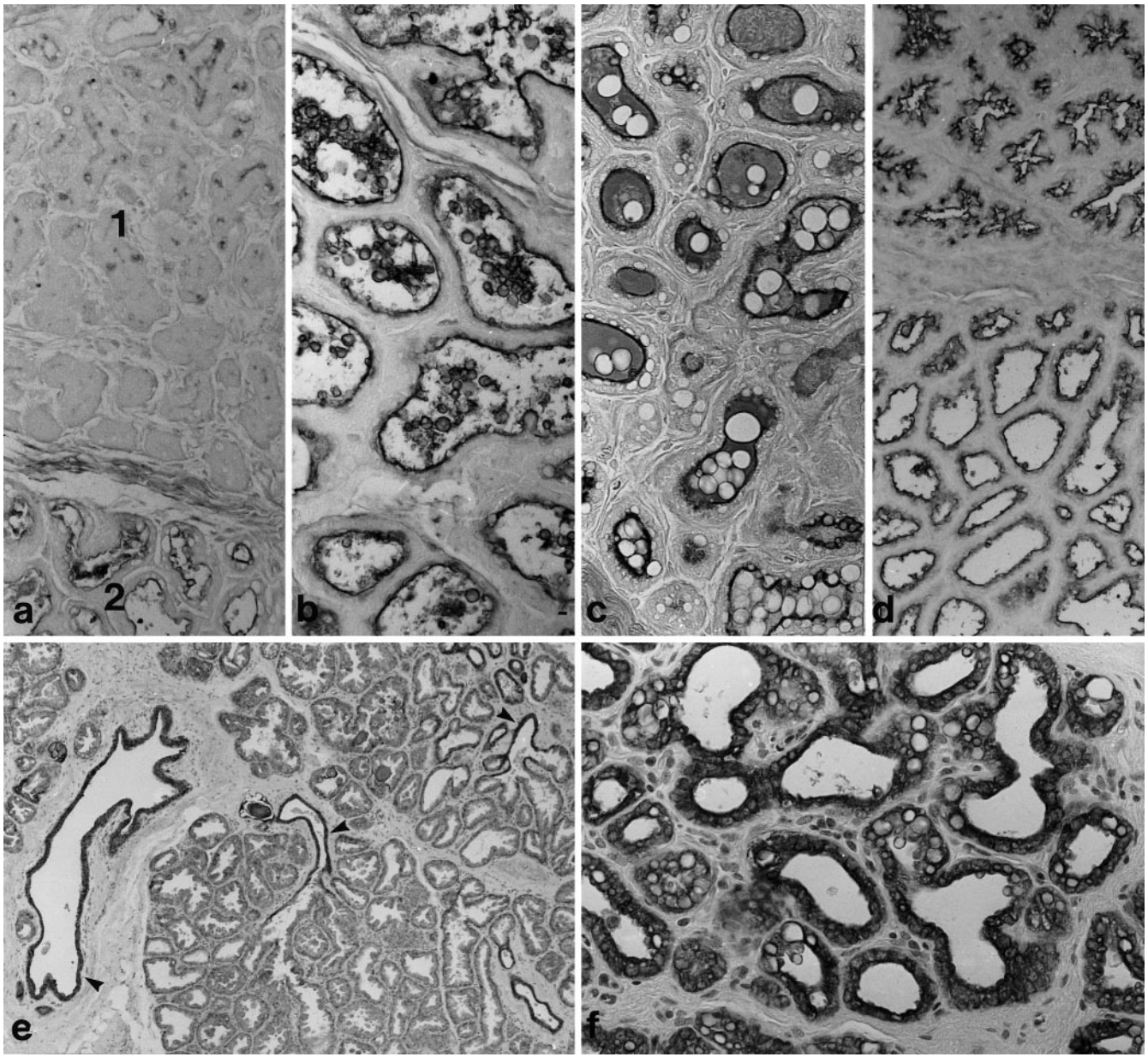

Fig. 3 a–d PNA binding in the lactating mammary gland. **a** Type 1 *(1)* and type 2 (*2*) lobules; in the type 1 lobule, note the increasing PNA-binding intensity with increasing development of the alveoli, marked by the increasing width of the lumen (from *below* to *above)*. x110. **b** Type 2b lobule with relatively small or medium-sized MFG. x220 **c** Type 2 lobules with variably sized MFG. x220. **d** Alveoli in a type 2a lobule *(above)* and a type 2c lobule *(below)*. x220. **e,f** CK 19 immunoreactivity. **e** Typical reaction pattern with strong reactivity in intra- and interlobular ducts (*arrowheads*). x44 **f** Type 2b lobule with positive reactivity in the secretory cells. x220

in more advanced alveoli of these lobules with a wider lumen. The contents of these vesicles display a striking structural pattern (see Fig. 5a, c); on emerging from the Golgi apparatus, the contents are initially dense and homogeneous but later become transformed into densely packed threadlike structures of 25–30 nm in thickness and are usually found both cross- or longitudinally sectioned in the vesicles. During this process, the vesicles increase in size and can attain a width of 0.6–0.65 µm. In these somewhat wider alveoli, the apical cytoplasm forms small or medium-sized protrusions that are filled with glycogen and that obviously can be pinched off (see Fig. 5b). The material in the alveolar lumen is usually eosinophilic and strongly PAS-positive (Fig. 1c) and does not contain typical casein micelles in transmission electron-microscopical preparations, but a fine particular matter (see Fig. 5a; the diameter of the irregularly shaped, non-sharply delineated particles is 10–20 nm). The lectins tested usually did not bind to the epithelia of the alveoli in type 1 lobules (Table 4). Moreover, in the case of PNA, which binds strongly to the mature alveoli (Fig. 3b–d), no binding is found in the immature tubular alveoli with a narrow lumen, whereas those with a

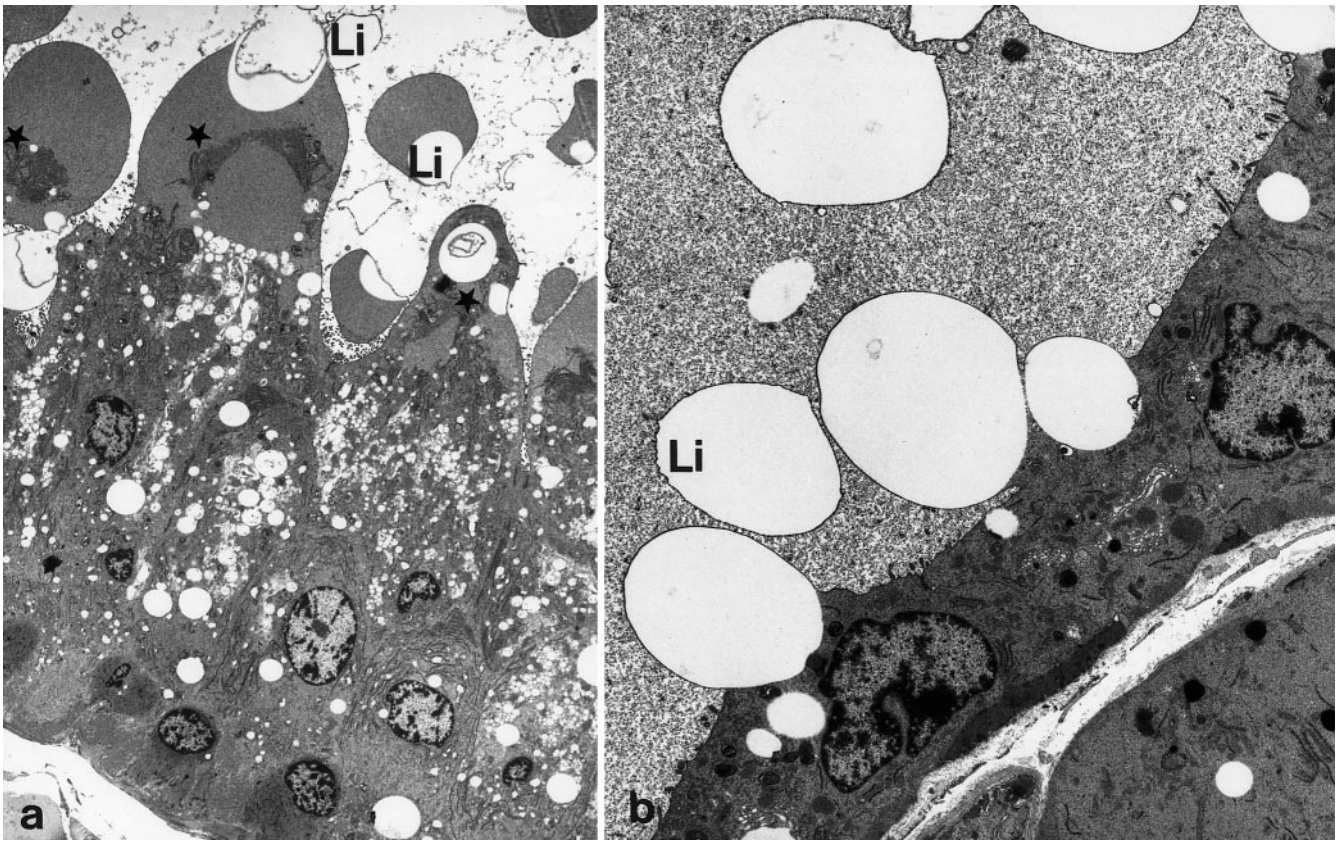

Fig. 4 a,b Transmission electron microscopy. **a** Low-power magnification of an alveolar wall in a type 2a lobule; note the apical protrusions (*stars*), well-developed Golgi apparatus, and protein vesicles and lipid droplets (*Li*), which are relatively small. x1554. **b** Low-power magnification of an alveolar wall of a type 2b lobule; note the large lipid droplets without crescents (*Li*). x3766

wider lumen show weak to medium-strong binding at the apical membrane (Fig. 3a). Myoepithelial cells are present and also contain numerous glycogen particles.

Type 2

This is the most common type of lobule and consists of alveoli actively producing and secreting protein and lipid. Concordant with a functional state of active secretion, PCNA-positive nuclei, mitotic or apoptotic figures and TUNEL-positive nuclei are rare in type 2 lobules. Proliferating cells have been observed with a frequency of usually 2–3 per section of a lobule and not exceeding about 10 (Fig. 2f). Cells with apoptotic nuclei occur in even smaller numbers, viz., 1–3 per lobule section (Fig. 2d). The glandular epithelial cells do not express CK 7, and only regionally CK 19. In one animal studied, most alveoli in the type 2 lobules were CK 19-positive (Fig. 3f). The alveoli contain a basal layer of myoepithelial cells that are strongly stained by anti-CK 14. Interestingly, in some type 2 lobules, only the base of the epithelium is positive for CK 19 in a peculiar small punctuate staining pattern. It remains uncertain whether this reaction occurs in myoepithelial cells or in the area of the basal folds (see below) of the glandular cells in which cytoskeletal filaments occur at the electron-microscopic level.

In alveoli of type 2, the apical intercellular junctions consist of tight junctions, intermediate junctions, and desmosomes. Single gap junctions and small desmosomes have been observed laterally. The basal cell membrane very often forms densely spaced microfolds that are particularly well developed opposite blood capillaries (see Fig. 6a). The distribution of the cytoskeleton is difficult to reconstruct on the basis of transmission electron- microscopical preparations. Cytoskeletal components have been mainly observed in the cellular periphery in the form of small bundles of intermediate filaments (10–12 nm) and thin filaments

Fig. 5a–f Transmission electron microscopy. Glycogen and secretory granules. **a–d** Details of the secretory epithelial cells in advanced alveoli of type 1 lobules. **a** Apices with abundant glycogen (*Gl*) and secretory granules (*arrows*). x15 300. **b** Small apical protrusions with glycogen (*Gl*) and small lipid droplets (*Li*). x36 609. **c** Secretory granules, some of which still have dense homogeneous regions (*arrows*), whereas others contain exclusively densely packed filamentous material. x66 654. **d** Protein vesicles attached to the apical cell membrane with intercalated dense material (*arrows*). x66 654 *L* Lumen. **e–f** Secretory cells of type 2 lobules. **e** Golgi apparatus (*G*) with typical protein vesicles (*P*). x20 700. **f** Lipid droplet (*Li*) with lamellar material at its periphery (*arrow*), and a protein (*P*) vesicle with loosely arranged small and medium-sized micelles. x90 293

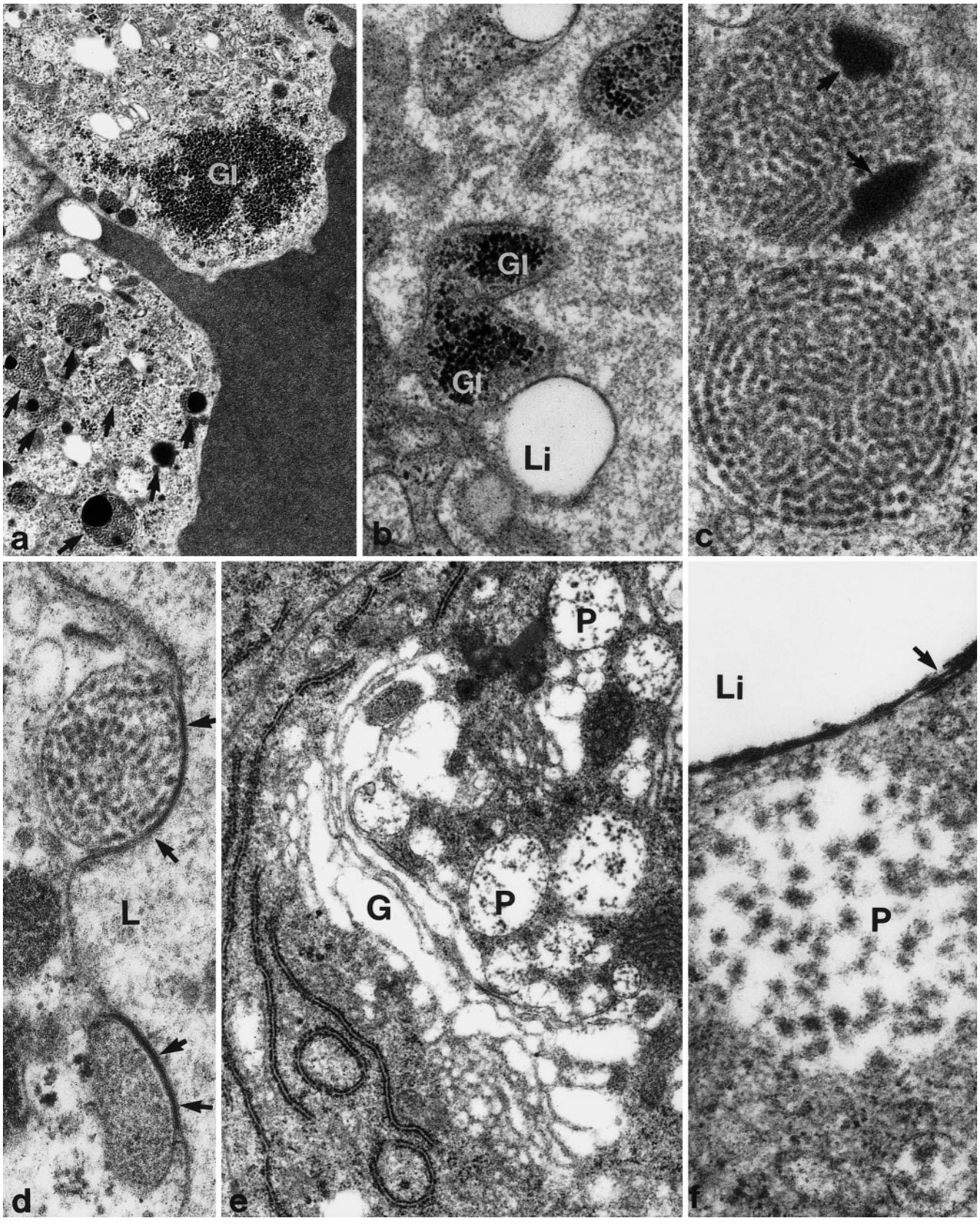
Gl
a
Gl
Gl
Li
b
c
L
d
P
G
P
e
Li
P
f

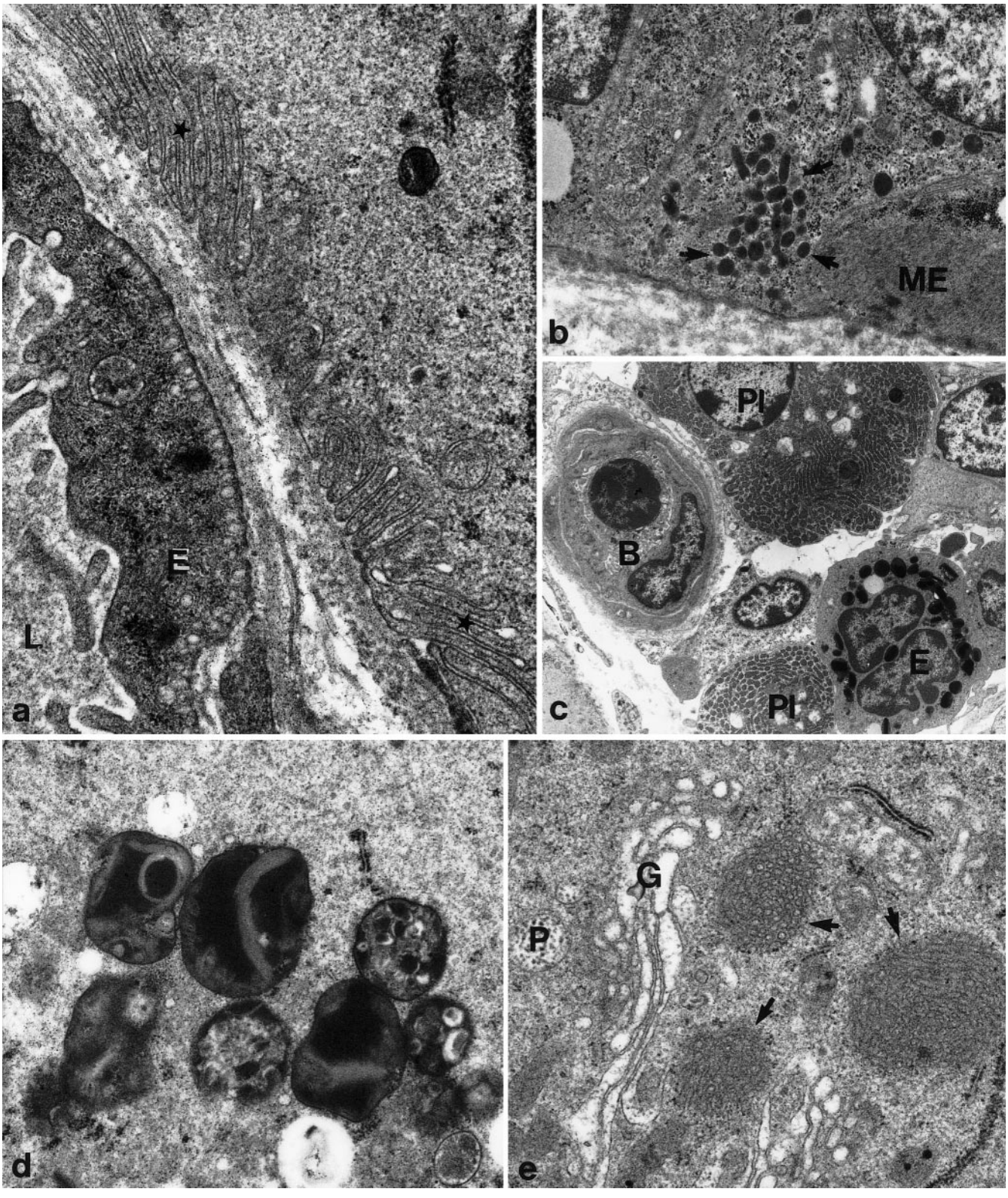

Fig. 6a–e Transmission electron microscopy. Lactating epithelial cells in lobules of type 2. **a** Abundant membrane folds of the basal cell membrane (*stars*) opposite a blood capillary (*L* capillary lumen, E endothelial cell of the capillary). x36 924. **b** Small dense granules (*arrows*) near the basal cell membrane (*ME* myoepithelial cell). x15 286. **c** Intralobular connective tissue with two plasma cells (*Pl*) and one eosinophil (*E*). *B* Blood capillary with lymphocyte in the lumen. x3900. **d** Lysosomal bodies in the supranuclear cytoplasm. x20 700. **e** Bodies composed of tubular structures (*arrows*) near a Golgi apparatus (*G*). *P* Protein vesicle. x26 560

Table 4 Lectin binding in alveoli, MFGM, and ductular epithelia; the reaction is confined to the apical cell membrane [(+) faint, + weak, ++ medium, +++ strong]

	Lobules type 1	Lobules type 2	Lobules type 3	MFGM	Interlobular ducts
WGA	–	–/(+)	(+)	–	–/(+)
RCA I	–	+/++	+	+	+
HPA	–	(+)/++	+	(+)	(+)
UEA I	–	(+)	–	–	(+)
Con A	–	(+)	(+)	–	(+)
PNA	–/(+)/+	+++	++	++	++

(5–6 nm), the latter being associated with the apical membrane and microvilli and with the basal lamellae. Microtubules have been observed mainly in the neighborhood of centrioles radiating into the cellular periphery. Myoepithelial cells are interconnected with the glandular epithelial cells by prominent desmosomes and among themselves by desmosomes and gap junctions, which, as in other species (Mepham 1987), couple these cells electrically.

Among type 2 lobules, three subtypes may be distinguished. These can be correlated with different phases of the secretory process.

Type 2a

The secretory portions have a prismatic epithelium 30–35 µm high and a comparatively narrow lumen with an irregular outline (Fig. 1e, f). The PAS reaction is confined to the apical membrane of the epithelial cells (Fig. 2a). In the light microscope, these protrusions, when fully developed, are eosinophilic and often contain a small lipid droplet; in the electron microscope (Fig. 4a), they have a smooth surface and are composed of fine flocculent material and contain small 1–4 µm, occasionally up to 10 µm lipid droplets, single ribosomes, single RER cisterns, individual protein vesicles, or one or two lysosomes. Such apical protrusions presumably pinch off and can fill the lumen with 10- to 15-µm-wide globular bodies, only some of which are occupied by a lipid droplet (Figs. 1g, 4a). Furthermore, casein micelles can be found (see Fig. 4b and Fig. 9a) measuring 35–90 nm (rarely up to 120 nm) in diameter in the lumen. When the apical protrusions are less prominent, they form microvilli and contain single smooth and coated vesicles, centrioles, abundant protein vesicles, and also small lipid droplets. The protein vesicles contain loosely distributed 30- to 90-nm particles (Fig. 5e, f) that are presumably casein micelles in various stages of formation. Outside the apical protrusion, the cytoplasm of all secretory epithelial cells is characterized by abundant cisterns of the RER, an extended supranuclear Golgi apparatus, many small mitochondria, protein vesicles, and lipid droplets of various sizes (Figs. 1e, 4a). The number of lipid droplets and secretory protein vesicles varies among the cells. The granules release their contents by exocytosis. Before opening up, the membrane of the granules attaches to the apical cell membrane; dense material, which is intercalated between cell membrane and granule membrane, apparently contributes to this attachment process (Fig. 5d). The smallest lipid droplets occur among RER cisterns in the basal part of the cells; they are larger in the supranuclear cytoplasm. Rarely, we observed medium-sized lipid droplets arranged in a baso-apical direction and obviously fusing with each other. Surprisingly, the cells often contain, in their supranuclear cytoplasm, several membrane-bounded large (diameter 0.7–1.3 µm) organelles with heterogeneous contents (Fig. 6d); these are apparently lysosomes and regularly display myelin figures or comparable stacks of membranous material. Near the large Golgi apparatus (Fig. 5e), numerous protein vesicles, single multivesicular bodies, and densely packed tubular profiles (diameter 0.75 to 1.2 µm) of an unknown nature and without a surrounding membrane may occur (Fig. 6e). The apical cell membrane forms single microvilli, which, however, disappear when the apical protrusions are fully developed. In the electron microscope, the apical membrane is covered by a fine glycocalyx that, in the light microscope, is PAS-positive (Fig. 2a) and also stains with Alcian blue; among the lectins tested, PNA binds strongly to the apical cell membrane (Fig. 3b–d), RCA I binds with medium intensity, whereas the other lectins (HPA, WGA, ConA, UEA I, RCA I) bind only weakly or very weakly (Table 4).

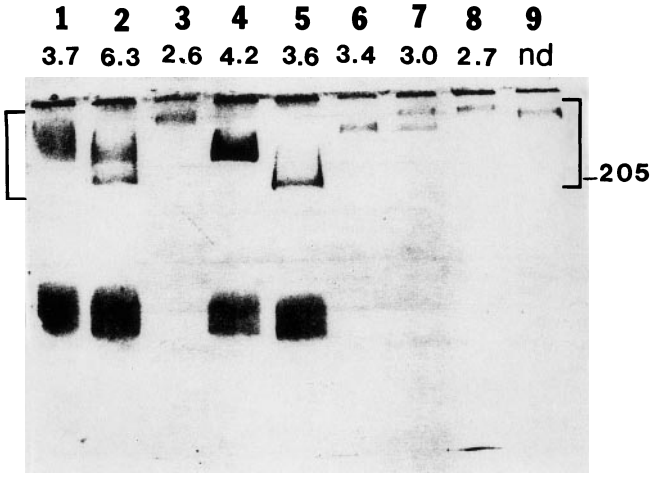

Fig. 7. SDS-gel showing the electrophoretic separation of the mucins in the MFGMs from 9 *(lanes 1–9)* different African elephant cows. *Brackets* define the polymorphic bands of MUC1. Molecular weight is indicated *right*. The protein content of each milk sample is indicated *below* each lane number (*nd* not determined). Note the strong stain outside the MUC1 bands in *lanes 1, 2, 4, 5*. Silver stain

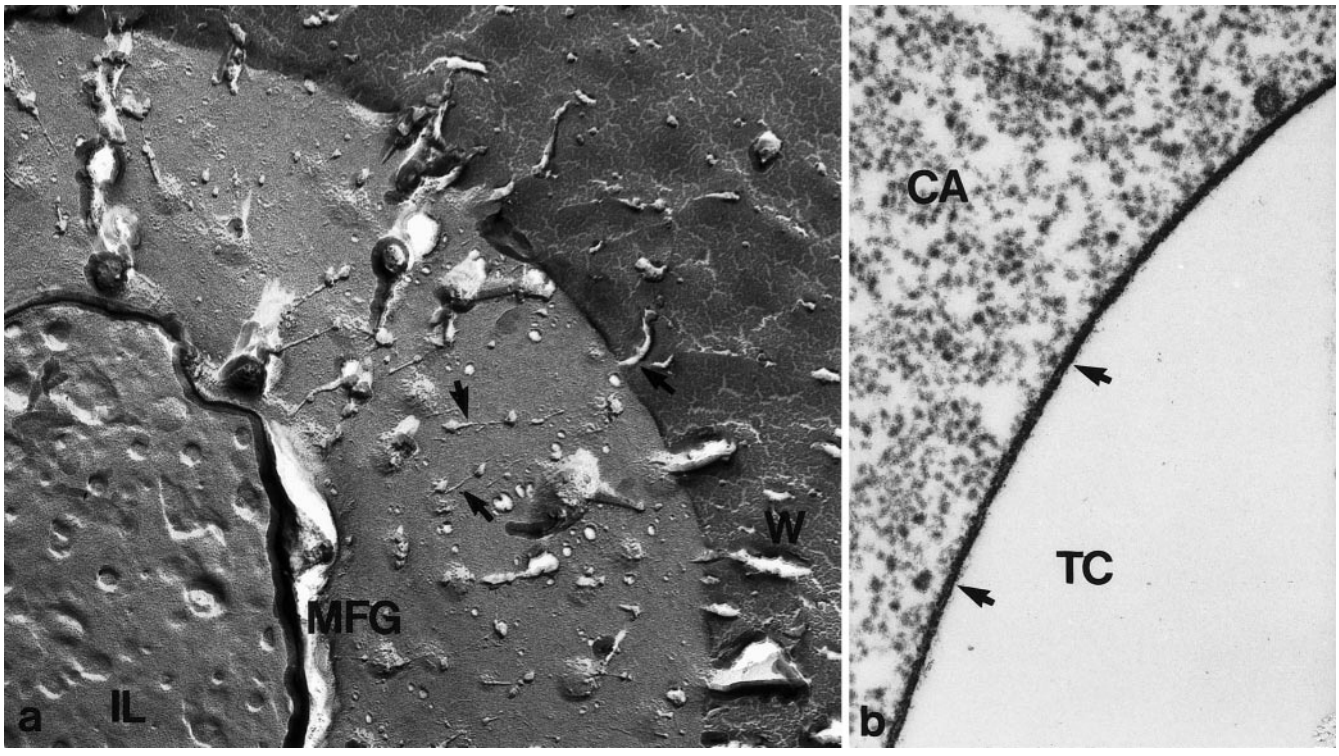

Fig. 8a,b Surface of the MFGMs. **a** Freeze-etch preparation of milk expressed manually from the gland (*MFG* milk fat globule, *arrows* mucin filaments extending from the outer leaflet of the MFGM, *IL* inner leaflet with impressions of the lens-shaped domains under the unit membrane, *W* water phase). x48 600. **b** Transmission electron-microscopical preparation of an MFG of alveolar milk, the proteinaceous coat (*arrows*) of which is not yet divided into lens-shaped domains; the surface coat is homogeneous (*TC* triglyceride core of the MFG, *Ca* casein micelles). x36 600

Type 2b

Type 2b alveoli have wider lumina and usually only cuboidal or low-prismatic epithelia of 10–15 µm height (Fig. 1h). The lumina contain numerous fat globules and eosinophilic granular material, corresponding to the casein micelles (Figs. 4b, see Fig. 9a), which measures 35–90 nm (rarely up to 130 nm) in diameter. Several lumina contain densely packed parallel threadlike formations with an electron-transparent core and a diameter of 30 nm per thread (Fig. 9b); these stain weakly with Alcian blue and PAS. The epithelial cells contain relatively large (5–15 µm in diameter) lipid droplets, which usually do not pinch off with a prominent apical protrusion but originate from a straight apical membrane (Fig. 4b), which again is PAS-positive (Fig. 2a) and strongly binds PNA (Fig. 3b, c). The intraluminal MFGs measure 5–25 µm in diameter, the majority having a diameter of 10–15 µm. They are larger than those within the cells, indicating that fusion of MFGs may occur in the alveolar lumen. These intra-alveolar MFGs rarely have cytoplasmic crescents; their membrane (MFGM) is also PAS- and PNA-positive (Fig. 3b, c) and also stains with Alcian blue. The MFGM apparently transforms rapidly; the proteinaceous coat between the lipid core and unit membrane is initially uniform and of medium density (see Fig. 8b); it becomes very dense and divides into small circular domains of 50–90 nm in diameter, but occasionally up to 160 nm (see Fig. 9a). Protein vesicles are comparatively rare. In alveoli of this type, the basal cell membrane forms a few microfolds. It is noteworthy that the basal cytoplasm often contains small accumulations of electron-dense granules near the basal cell membrane with a long diameter of 300–320 nm and a short diameter of 120–135 nm (Fig. 6b). In single alveoli, 80- to 100 µm wide basophilic bodies, presumable corpora amylacea, can be found. Proliferating and apoptotic cells are rare in these lobules (Fig. 2d, f).

Type 2c

This type is characterized by relatively wide alveoli with cuboidal or even flattened epithelia, 5–10 µm high, which shows no signs of active secretion. The lumina are largely devoid of MFG and proteinaceous matter (Fig. 1i).

Type 3

This type of lobule is not common and is characterized by alveoli with cuboidal pale epithelial cells with strikingly large lipid droplets (diameter 15–25 µm) and similarly sized MFG in the lumen (Fig. 1j). Several alveoli in such lobules show signs of disintegration with broken alveolar

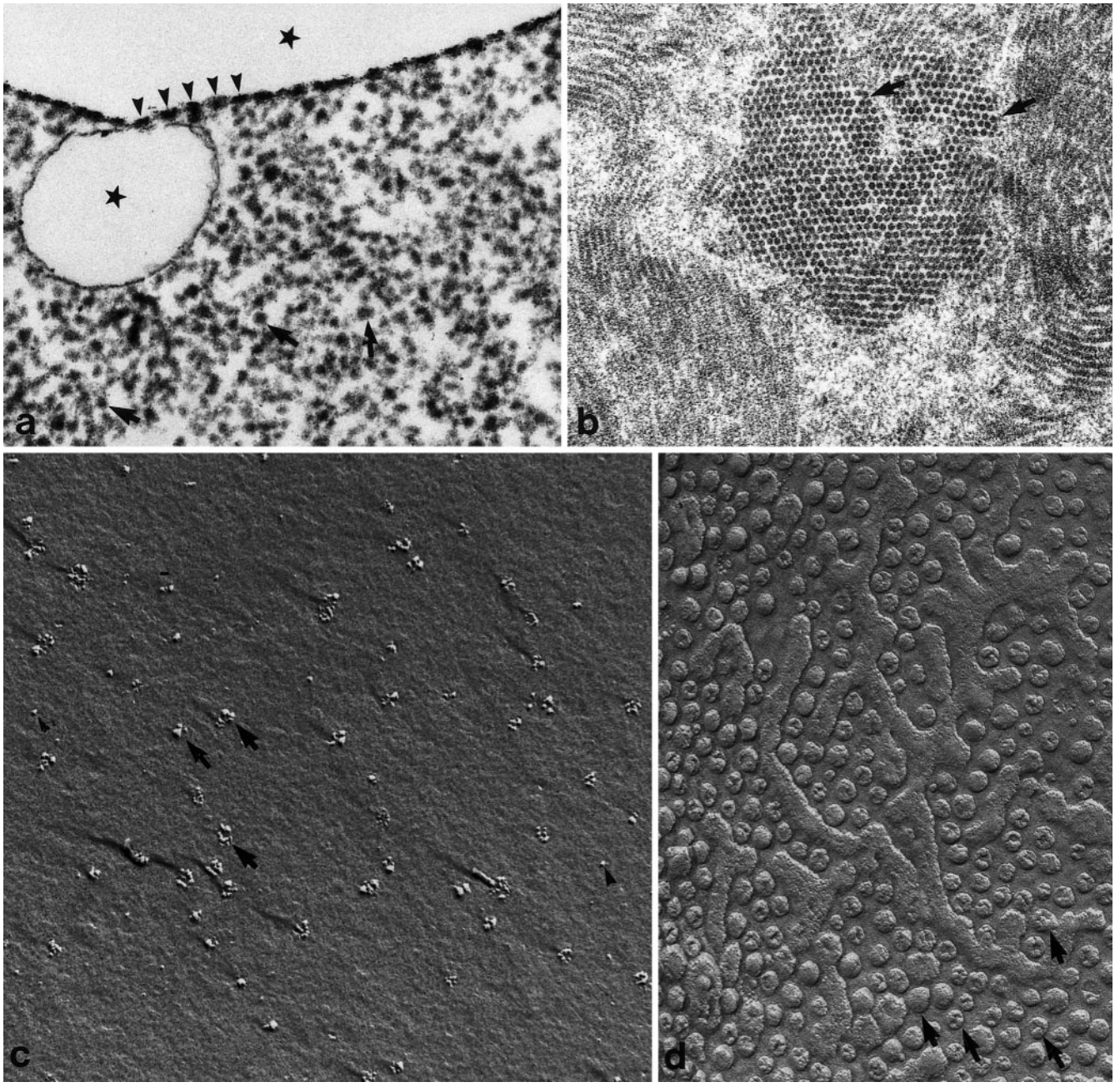

Fig. 9a–d Transmission electron microscopy (**a,b**), freeze-fracture (**c**), and freeze-etch (**d**) preparations of the milk of the African elephant. **a** Alveolar milk with abundant casein micelles (*arrows*) and part of a small and a large MFG. Note that the proteinaceous coat of the membrane of the large MFG is divided into electron-dense lens-shaped domains (*arrowheads*); the triglyceride core (*stars*) of the MFG appears to be empty. x49 950. **b** Alveolar milk with densely packed filamentous structures, which in cross-sections have an electron-transparent core (*arrows*). x36 925. **c** Milk manually expressed from the mammary gland; note the casein micelles (*arrows*) and small single particles (diameter about 4 nm, *arrowheads*) possibly corresponding to whey proteins. x48 600. **d** MFGM; inner leaflet exhibiting lens-shaped domains (*arrows*) and worm-shaped structures. x48 600

walls; the nuclei of the partly fragmented epithelial cells are often relatively dense. This observation is particularly prominent in sections stained by the Feulgen reaction. Several nuclei of epithelial cells in these lobules show ultrastructural characteristics of programmed cell death, such as the condensation of chromatin into “crescents”, nuclear fragmentation, and apoptotic bodies. The alveolar lumina contain single disintegrated epithelial cells and neutrophil granulocytes, as identified by the typical nuclear structure and characteristics granules. Both epithelial cells and neutrophil granulocytes are frequently stained by the TUNEL procedure (Fig. 2c). In such alveoli, macrophages can be observed containing phagocytosed remnants of epithelial cells.

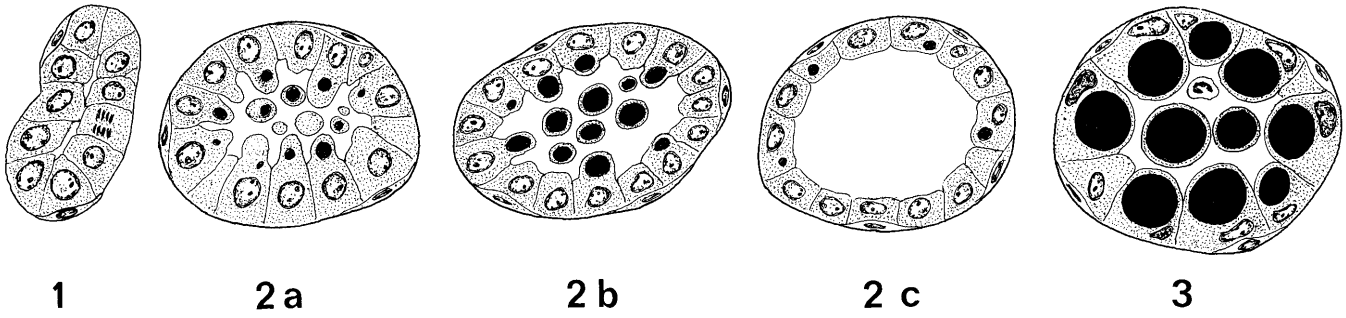

Fig. 10 Schematic drawing of typical alveoli in lobules of types *1*, *2a*, *2b*, *2c*, and *3*. These alveoli are interpreted as representing a series of increasing differentiation and finally degeneration (type *3*). Alveoli with intermediate characters can also be found

Occasionally, lobules are observed containing alveoli characteristic for lobules of type 1, 2, or 3. Lobules are consistently found with considerable numbers of the immature type 1 alveoli, and substantial numbers of type 3 alveoli at their periphery (Fig. 2e).

The teat

The teats contain several teat canals, in which two segments can be distinguished: the distal segment is several millimeters long, narrow, and lined by a multi-layered, flat, slightly cornified epithelium. The much longer proximal segment is wide and lined by a two-layered epithelium of basal myoepithelial cells and cuboidal apical cells. A striking characteristic of this segment are the numerous densely spaced folds of its wall. The folds can be thin and mainly formed by the epithelium or wider and enclosed with a substantial connective-tissue core.

Milk

Representative gel-electrophoretic data displaying MUC 1 band patterns for the nine African elephant milk samples are shown in Fig. 7. Variation in mobilities (molecular masses) of the bands is evident. Samples in lanes 2 and 7 show the characteristic double-band pattern varying in size because of genes from the two parents. Mucin bands of elephant milk range from about Mr 200 000 upward. Surprisingly, the elephant milk samples fall into two groups, based on the data of Fig. 7. Those in lanes 1, 2, 4, and 5 stain more heavily, have mucin bands showing greater mobilities than the samples in lanes 3 and 6–9, and have higher protein contents.

The protein content of the individual milk samples varied between 2.6% and 6.3% and is listed in percent below the lane number in Fig. 7. The striking protein bands in rows 1, 2, 4, and 5 are found relatively high in the running gel and are relatively wide, suggesting that they are glycoproteins.

Freeze-fracture, freeze-etching, and transmission electron-microscopical preparations

In freeze-etched preparations of MFGs the surface of the globules bears 100–150 nm-long branched filaments (Fig. 8a) that are anchored in the unit membrane of the MFGM. The inner layer of the MFGM, beneath the unit membrane, is termed the ‘proteinaceous coat’, which in the African elephant is composed of circular lens-shaped domains (Fig. 9d) measuring 40–90 nm in diameter and with occasional indications of 15-nm subunits. Partly anastomosing worm-shaped structures occur that are regularly about 1 µm long and 60 nm wide (Fig. 9d); these may either be remnants of an originally uniform proteinaceous coat (see Fig. 8b) or indicate fusion of the lens-shaped domains. Areas with a paracrystalline substructure, as described in several other species (Buchheim 1982b), have not been found in the proteinaceous coat of the African elephant. In freeze-fracture preparations, casein micelles measure about 40–80 nm in diameter.

The long filaments at the surface of the MFGM were not detectable in sectioned materials of milk samples; instead, a dense glycocalyx (thickness about 15 nm; Fig. 8b) was visible. The unit membrane and the lens-shaped domains of the proteinaceous coat were also clearly visible in transmission electron-microscopical preparations (Fig. 9a). Casein micelles (Fig. 8b) were often comparatively homogeneous; higher magnifications, however, revealed that they were composed of subunits (5–6 nm in diameter), as observed in sectioned material of several other mammals (Wooding 1977; Jensen et al. 1995). The diameter of the micelles measured 40–90 nm (occasionally up to 130 nm) in transmission electron-microscopical preparations.

Discussion

The present study has shown that the lactating mammary gland of the African elephant corresponds in its fundamental histological and ultrastructural organization to that described in other placental mammals (Dabelow 1957; Wooding 1977). The present investigation, however, provides an

unusually dynamic picture of the lactating tissue in the African elephant, including the formation of new lobules and the occurrence of programmed cell death of entire groups of alveoli among actively secreting lobules. This allows a new classification of the lobules based on a variety of histological, histochemical, immunohistochemical, and ultrastructural features (Fig. 10). The observations of the mammary gland of the elephant underline that the lobule is not only the structural but also the functional unit of the mammary gland (Dabelow 1957; Mepham 1987). The variability of the lobular structure in the African elephant may be hypothetically correlated with the long duration of the lactating period (Perry 1953), leading to exhaustion to the lactating epithelia and requiring recruitment of new lobules. Although it was not possible to determine how long the lactation period had been going on in the individual animals studied, all of them had been producing milk at least for several months; thus, we consider that we can provide a report on the typical situation in the fully lactating mammary gland.

In the following discussion, emphasis is placed upon the functional interpretation of the different types of lobules. Although the division into several types of glandular lobules remains provisional, it appears to be useful to classify the typical morphological differences of the alveoli, especially since they can be associated with various functional parameters. Naturally, lobules with transitory characters occur frequently.

The ductular and tubular-alveolar structures and the connective tissue in type 1 lobules appear to represent an immature state of differentiation. Mitotic figures are common, and the PCNA immunoreaction is positive in comparatively numerous nuclei. Interestingly, such immature alveolar and ductular structures immunoreact for CK 19, a marker of inter- and intralobular ducts, indicating their origin from small interlobular ducts. The apical cell membrane of the immature alveolar epithelial cells only weakly expresses carbohydrate components; this is especially evident in the case of PNA-binding sites, which mark the apical membrane of fully secreting cells. The strong PNA binding of the apical membrane of the lactating epithelia and of the MFGM in the African elephant agrees with corresponding observations in the mammary gland of other mammals including human (Horisberger et al. 1977; Schinko et al. 1987; Buchheim et al. 1987; Welsch et al. 1988). There is probably more variation among different species with respect to the binding intensity of other lectins; however, the sugars detected by lectin binding in the African elephant at the apical membrane of the lactating cells agree with those listed for some mammals by Patton et al. (1989).

Secretory epithelial cells of advanced alveoli in type 1 lobules not only form a special type of secretory granule (see below), but also apparently pinch off small portions of cytoplasm containing abundant glycogen particles. This observation may explain in part the PAS staining of the luminal contents of such alveoli and may possibly be correlated with the finding that the sugar content of the milk of the African elephant is much higher during the first 2–3 months of lactation than during the rest of the long lactating period (McCullagh and Widdowson 1970). In the Indian elephant, the sugar levels of the milk appear to be generally high, whereas the lipid concentrations remain relatively low (Peters et al. 1972). The strong PAS positivity of the lumen and the cells may also depend on the immunoglobulins (IgA) secreted into the lumen. The presence of IgA in these lobules is highly probable, since abundant plasma cells occur in the peri-alveolar connective tissue. Furthermore, other glycoproteins may be present in the luminal milk, since the electrophoretic observations obtained from four milk samples suggest the presence of a glycoprotein (other than the MFGM mucins) in milk. The significance of the high content of carboxylated and sulfated glycosaminoglycans in the connective tissue of lobules of type 1 is not fully elucidated but the correlation with an immature state of the epithelium is striking and supports the view that glycosaminoglycans and proteoglycans can promote the growth and differentiation of epithelia (see Erlinger et al. 1990).

Type 2 lobules contain alveoli actively synthesizing and extruding their secretory products. The three tentatively described subtypes probably represent different physiological phases of the glandular epithelium. In type 2a lobules, the alveolar secretory cells are particularly tall because of a well-developed apical protrusion and contain numerous protein vesicles and predominantly small and medium-sized lipid droplets. The MFGs are secreted in an apocrine fashion; it is, however, striking that the lipid droplets often occupy only a small part of the apical protrusion and that apical protrusions are sometimes pinched off without lipid droplets. This observation is reminiscent of apocrine phenomena as described in glands of the reproductive tract (Aumüller and Seitz 1990; Seitz et al. 1990; Wilhelm et al. 1998). Possibly, in the mammary gland of the elephant, the apical cytoplasm discharged by the apocrine mechanism contains an important enzymatic component of the milk. The tall secretory cells display numerous lysosomal bodies in their cytoplasm, indicating that these cells have the ability to degrade secretory materials and that an imbalance may occur temporarily between synthesis and degradation in cells with a prominent apical protrusion. Myelin figures within the lysosomal bodies indicate membrane turnover. Lysosomal bodies are common in certain other apocrine glands, e.g., in the human axilla (Montagna et al. 1992).

In type 2b lobules, the glandular cells secrete MFG that are generally larger than those in type 2a lobules and that lack any prominent cytoplasmic crescents. Protein seems to be produced in reduced quantities, as judged by the numbers of organelles and secretory vesicles. In alveoli of type 2b lobules, the MFG are discharged from cuboidal or even low prismatic secretory cells devoid of protrusions. Type 2c appears to represent a phase in which the milk has been released from the alveoli and the epithelial cells are relatively inactive.

Type 3 lobules are regarded as representing a phase of degeneration, with apoptotic cell nuclei and a cytoplasm relatively poor in organelles. Apoptosis has been repeatedly described as the principal mechanism of involution of the mammary gland in placental mammals (Walker et al. 1986; Li et al. 1997). In the sheep (Tatarczuch et al. 1997), the

apoptotic cells contain “stasis vacuoles”, which are different from the large lipid droplets seen in the elephant. In the sheep mammary gland, a leukocytic infiltration occurs during early involution, comparable to the presence of neutrophils in the degeneration alveoli of type 3 lobules in the elephant.

Apoptotic phenomena and proliferative processes appear to be functionally coupled in developing mammary glands. In the mouse, Humphreys et al. (1996) have postulated that apoptosis is involved in the morphogenesis of the mammary gland. These authors have found defined zones with significant apoptosis in proliferating end buds. Although the proliferating and the fully lactating mammary glands are not directly comparable, proliferations and apoptosis may be coupled by unknown signals leading to the formation of new lobules during the long lactation period of the African elephant. In addition to this process, which involves whole lobules, the present study has shown that single glandular cells are replaced in actively secreting lobules.

The findings regarding the protein (casein) vesicles in the lactating cells and the intraluminal protein particles, and the gel-electrophoretic observations do not provide a uniform picture. The protein particles in advanced alveoli of type 1 lobules exhibit a striking morphological pattern not to be found in other mammals. Protein(s) different from casein are possibly present in these granules. In the lumen of such alveoli, small particles of 15–20 nm in diameter occur; these are different in size and morphology from those in alveoli of type 2 lobules. It may be speculated that, among these particles, fixation-induced aggregates of immunoglobulins or secretory compounds are also found; these aggregates may occur in colostral milk or together with IgA (Mepham 1987).

In actively secreting cells, the intracellular protein granules contain scattered small (30–90 nm) particles, which probably correspond to various stages of micelle formation. The intraluminal protein (casein) particles show a variable size ranging from 35 nm to 90 nm and rarely to 130 nm. With respect to size, the casein micelles of the African elephant are similar to those of humans, slightly smaller than those of cows, and considerably smaller than those of horses (Rüegg and Blanc 1982; Welsch et al. 1988). The micellar fine structure is borne out particularly clear in the freeze-fracture preparations. The nature of the threadlike or tubular protein formations in the milk of the African elephant remains unknown. The general protein content of this milk is variable (McCullagh and Widdowson 1970; this study). A morphological correlate to the high water content of the milk are the unusually well-developed basal membrane folds in the actively lactating glandular cells. Together with abundant mitochondria, they suggest considerable fluid and electrolyte transport. Moreover, the often strikingly wide lymphatic vessels point to a considerable fluid turnover. No specific biochemical data are so far available on the proteins in the milk of the elephant; more especially, the principal protein, casein, has not been studied.

The structure of the MFGM of the African elephant displays the same basic elements as in other mammals (Buchheim et al. 1987). In the proteinaceous coat, the absence of paracrystalline components, which apparently represent the enzyme xanthine oxidase in bovine MFGMs (Buchheim 1982b), is striking. The fragmentation of the proteinaceous coat into lens-shaped domains of uniform size is also peculiar. The transformation of an initially homogeneous proteinaceous coat into these domains appears to take place rapidly, since they are present in the majority of alveolar MFG. In freeze-etch preparations, the surface of the MFGM of the African elephant bears filamentous structures that correspond to membrane-anchored mucins (Patton et al. 1995). Such filaments have been detected in several mammalian species but are absent in ruminants under the technical conditions employed in this study. The length (100–150 nm) of the filaments on the elephant MFGMs is smaller than that on human and equine MFGMs, which measure about 500 nm. Nevertheless, the electrophoretic data show that the mucins involved belong to the MUC 1 group (Patton et al. 1995). The availability of milk samples from nine female African elephants has enabled an evaluation of the polymorphic mucin MUC 1 in this species. Because of variable numbers of a tandemly repeated sequence containing 20 amino acids, the inherited MUC 1 genes, viz., one from each parent, may give rise to mucins of different molecular masses (Patton and Patton 1990; Patton et al. 1989, 1995). To date, this polymorphism has been confirmed in the human, chimpanzee, rhesus monkey, horse, and cow (Patton et al. 1989) and is also present in the African elephant, but is absent in the mouse (Spicer et al. 1991).

Although mucin bands of bovine milk exhibit mobilities between Mr 160 000 and 200 000, the mucin bands of the African elephant MFGs range from about 200 000 upwards. Mobilities of mucin bands in mare milk samples are also above Mr 200 000 (Welsch et al. 1988; Patton et al. 1989); this may point to a closer phylogenetic proximity between Proboscidea and Perissodactyla than between Proboscidea and Articodactyla.

The reason for the two groups of milk as found by gel electrophoresis is not known. However, significant changes in the composition of milk with advancing lactation do occur. In the African elephant, an initially high content in carbohydrates and a steady increase in protein content with advancing lactation have been reported by McCullagh and Widdowson (1970). Unfortunately, the length of the lactation period in the elephants of this study has not been established. From differences in staining intensities and mobilities of the MUC 1 bands of the two groups of elephant milk, we suspect that the degree of glycosylation may be a contributing variable. In particular, greater sialylation may increase both the mobility and staining intensity of the bands (Huott et al. 1995).

Finally, the observation of small electron-dense granules near the basal cell membrane suggests the formation of a regulatory para- or autocrine factor, a possibility that has been considered before (see Mepham 1987) and that is presently under investigation in our laboratory.

Acknowledgements. The assistance of the National Parks Board of South Africa with respect to the collection of study material is gratefully acknowledged. D. Moss provided valuable technical assistance. We thank Prof. C. Baumrucker of the Pennsylvania State University for use of facilities in the analysis of elephant milk samples.

References

Aumüller G, Seitz J (1990) Protein secretion and secretory processes in male accessory sex glands. Int Rev Cytol 121: 127–231

Buchheim W (1982a) Aspects of sample preparation for freeze fracture/freeze etch studies of proteins and lipids in food systems. Food Microstruct 1: 189–208

Buchheim W (1982b) Paracystalline arrays of milk fat globule membrane-associated proteins as revealed by freeze fracture. Naturwissenschaften 69: 505–506

Buchheim W, Welsch U, Patton S (1987) Electron microscopy and carbohydrate histochemistry of the human milk fat globule membrane. In Hanson G, et al. (eds) Biology of human milk. Nestle-Workshop, Athens, April 1986

Dabelow A (1957) Die Milchdrüse. In: Bargmann W (ed) Handbuch der mikroskopischen Anatomie des Menschen, III/3. Springer, Berlin Heidelberg New York, pp 277–485

Dulbecco R, Unger M, Armstrong B, Bowman M, Syka P (1983) Epithelial cell types and their evolution in the rat mammary gland determined by immunological markers. Proc Natl Acad Sci USA 80 :1033–1037

Erlinger R, Schumacher U, Welsch U (199) Ultrastructural localization of glycosaminoglycans in the human mammary gland. Acta Histochem XL: 65–70

Feulgen R, Rossenbeck H (1924) Mikroskopisch-chemischer Nachweis einer Nukleinsäure vom Typus der Thymonukleinsäure und die darauf beruhende selektive Färbung von Zellkernen in mikroskopischen Präparaten. Z Physiol Chem 135: 203–248

Gavrieli Y, Sherman Y, Ben-Sasson SA (1992) Identification of programmed cell death in situ via specific labeling of nuclear DNA fragmentation. J Cell Biol 119: 493–501

Greyling MD, Aarde RJ van, Potgieter HC (1997) Ligand specificity of uterine oestrogen and progesteron receptors in the subadult African elephant *Loxodonta africana*. J Reprod Fert 109: 199–204

Horrisberger M, Rosset J, Vonlathen M (1977) Locating of glycoproteins on milk fat globule membrane by scanning and transmission electron microscopy using lectin labeled gold granule. Exp Cell Res 109: 361–369

Horwitz W (1975) In Horwitz W (ed) Official methods of analysis, 13th edn. Association of Official Analytical Chemists, Washington, D.C. 1975:251-292

Humphreys RC, Krajewska M, Krnacik S, Jaeger R, Weiher H, Krajewski S, Reed JC, Rosen JM (1996) Apoptosis in the terminal endbud of the murine mammary gland: a mechanism of ductal morphogenesis. Development 122: 4013–4022

Huott ML, Josephson RV, Hens JR, Rogers GW, Patton S (1995) Polymorphic forms of the epithelial mucin, PAS-I (MUC 1), in milk of Holstein cows. Comp Biochem Physiol 111B: 559–565

Jensen RG, Blank B, Patton S (1995) The structure of milk. Particulate consistents in human and bovine milks. In: Jensen RG (ed) Handbook of milk composition. San Diego, Academic Press, pp 50–62

Joshi K, Ellis JTB, Huges CM, Monaghan P, Neville AM (1986) Cellular proliferation in the rat mammary gland during pregnancy and lactation. Lab Invest 54: 52–61

Laemmli UK et al. (1970) Cleavage of structural proteins during the assembly of the head bacteriophage T4. Nature 227:680-685

Laws RM (1969) Aspects of reproduction in the African elephant *Loxodonta africana*. J Reprod Fertil Suppl 6: 193–217

Li M, Liu X, Robinson G, Bar-Peled U, Wagner KU, Scott-Young W, Hennighausen L, Furth PA (1997) Mammary-derived signals activate programmed cell death during the first stage of mammary gland involution. Proc Natl Acad Sci USA 94: 3425–3430

Mepham TB (1987) Physiology of lactation. Open University Press, Milton Keynes Philadelphia

McCullagh KG, Lincoln HG, Southgate DAT (1969) Fatty acid composition of milk fat of the African elephant. Nature 222: 493–494

McCullagh KG, Widdowson EM (1970) The milk of African elephant. Br J Nutr 24: 109–117

Moll R, Werner W, Franke W, Schiller DL (1982) The catalog of human cytokeratins: patterns of expression in normal epithelial, tumors and cultured cells. Cell 31: 11–24

Montagna W, Kligman AM, Carlisle KS (1992) Atlas of normal human skin. Springer New York

Morressey, JH (1981) Silver stain for proteins in polyacrylamide gels: a modified procedure with enhanced uniform activity. Anal Biochem 117: 307–310

Patton S, Huston GE (1986) A method for isolation of milk fat globules. Lipids 21: 170–174

Patton S, Patton RS (1990) Genetic polymorphism of PAS-I, the mucin-like glycoprotein of bovine milk fat globule membrane. J Dairy Sci 73: 3567–3574

Patton S, Huston GE, Jenness R, Vaucher Y (1989) Differences between individuals in high-molecular weight glycoproteins from mammary epithelia of several species. Biochim Biophys Acta 980: 333–338

Patton S, Gendler SJ, Spicer AP (1995) The epithelial mucin, MUC 1, of milk, mammary gland, and other tissues, Biochem Biophys Acta 1241: 407–423

Perry JS (1953) The reproduction of the African elephant (*Loxodonta africana*). Phil Trans R Soc [B] 237: 93–149

Peters JM, Maier R, Hawthorne BE, Storvik CA (1972) Composition and nutrient content of elephant (*Elephas maximus*) milk. J Mammal 53: 717–724

Purkis PE, Steel JB, Mackenzie IC, Nathrath WBJ, Leigh IM, Lane EB (1990) Antibody markers of basal cells in complex epithelial. J Cell Sci 97: 39–50

Romeis B (1989) Mikroskopische Technik, 16 edn. Urban & Schwarzenberg, Munich Vienna

Rüegg M, Blanc B (1982) Structure and properties of the particular constituents of human milk. A review. Food Microstruct 2: 25–47

Schinko I, Welsch U, Reyerman B (1987) Bindungsstelle von Lektinen an Milchdrüsenepithelzellen der Ratte sowie Aufnahme und intrazellulärer Transport von markiertem Weizenkeimagglutinin (WGA) nach Infusion in die laktierende Drüse. Verh Anat Ges 81: 6695–6697

Seitz J, Keppler C, Rausch U, Aumüller G (1990) Immunohistochemistry of secretory transglutaminase from rodent prostate. Histochemistry 93: 525–530

Skinner JD, Smithers RHN (1990) The Mammals of the Southern African Subregion. University of Pretoria, Pretoria

Spicer AP, Parry G, Patton S, Gendler SJ (1991) Molecular cloning and analysis of the mouse homologue of the tumor-associated mucin, MUC 1, reveals conservation of potential O-glycosylation sites, transmembrane and cytoplasmic domains and a loss of minisatellite-like polymorphism. J Biol Chem 266: 15099–15109

Tatarczuch L, Philip C, Lee CS (1997) Involution of the sheep mammary gland. J Anat 190: 405–416

Walker NI, Ellis JTB, Huges CM, Monaghan P, Neville AM (1986) Cellular proliferation in the rat mammary gland during pregnancy and lactation. Lab Invest 54: 52–61

Welsch U, Buchheim W, Schumacher U, Schinko I, Patton S (1988) Structural, histochemical and biochemical observations on horse milk-fat-globule membranes and casein micelles. Histochemistry 88: 357–365

Welsch U, Buchheim W, Schinko I, Jenness P, Patton S (1990) Histochemical and biochemical observations on milk-fat-globule membranes from several mammalian species. Acta Histochem XL: 59–64

Wilhelm B, Keppler C, Hoffbauer G, Lottspeich F, Linder D, Meinhardt A, Aumüller G, Seitz J (1998) Cytoplasmic carbonic anhydrase II of rat coagulating gland is secreted via the apocrine export mode. J Histochem Cytochem 46: 505–511

Wooding FBP (1977) Comparative mammary fine structure. Symp Zool Soc Lond 41: 1–41

Wu AM, Herp A (1985) A table of lectin carbohydrate specificities. In: Bög-Hansen TC, Breborowicx J (eds) Lectins IV. Gruyter, Berlin New York